Working Paper Series

WIF-17-002：Mar 2017

The Numerical Performance of Multilevel Monte Carlo Method Using Three Discretization Schemes

Hitoshi Inui *Center for Finance Research of Commerce,Waseda University*

Katsunori Ano *Department of Mathematical Sciences,College of Systems Engineering and Science, Sibaura Institute of Technology*

早稲田大学ファイナンス総合研究所

http://www.waseda.jp/wnfs/labo/labo3.html

The Numerical Performance of Multilevel Monte Carlo Method Using Three Discretization Schemes

Hitoshi Inui
Center for Finance Research of Commerce
Waseda University
Okuma Memorial Tower 1-6-1, Nishi-waseda, Shinjyuku-ku, Tokyo,
169-8050, Japan
h-inui@aoni.waseda.jp

Katsunori Ano
Department of Mathematical Sciences,
College of Systems Engineering and Science,
Sibaura Institute of Technology
307 Fukasaku Minami-ku, Saitama-city 337-8570, Japan
k-ano@shibaura-it.ac.jp

Abstract This study aims to numerically show the improvement in the strong and weak convergence of multilevel Monte Carlo method using the order 1.5 Taylor strong scheme. The multilevel Monte Carlo method, using the scheme, is tested for pricing eight options based on a geometric Brownian motion. The options are European vanilla, Asian, Lookback, Digital, Power, Rainbow, Cliquet, and Exchange option. In addition, the multilevel Monte Carlo method using the Milstein scheme is tested for pricing four Exotic options (Power, Rainbow, Cliquet, and Exchange) based on the geometric Brownian motion, and the multilevel Monte Carlo method using the Euler scheme is tested for European option based on a well-known stochastic volatility model. The model is the SABR model. Numerical results demonstrate that the multilevel Monte Carlo method, using the order 1.5 Taylor strong scheme, attains computational complexity reduction of 7-99.9% for the required five different accuracies, compared with other Monte Carlo methods. They also suggest that the strong and weak convergence of the multilevel Monte Carlo method using the order 1.5 Taylor scheme is the fastest, and that the multilevel Monte Carlo method has much better performance than the standard Monte Carlo method without depending on discretization schemes and models.

Keywords: Monte Carlo, multilevel Monte Carlo, strong Taylor scheme, computational complexity reduction, option pricing

1. Introduction

The Monte Carlo simulation is a useful and powerful numerical tool. It is popular in computational finance for financial derivatives pricing; however, its computational complexity may become too large for attaining the required accuracy. The Multilevel Monte Carlo (MLMC) method was proposed by Giles[3] to reduce this computational complexity.

This method has been actively studied. For example, representative variance reduction methods were applied in the MLMC method. (e.g., Antithetic variates method: see Giles and Szpruch[6] and Giles and Szpruch[7], Control variates method: see Nobile and Tesei[13], and Importance Sampling method: see Kebaier and Lelong[11]). In addition, the Quasi Monte Carlo method was also studied under the MLMC framework (see Giles and Waterhouse[4] and Dick, Kuo, Gla and Schwab[1]).

Let $\{S_t\}_t$ be a stochastic process driven by a stochastic differential equation (SDE) given

by

$$dS_t = \mu\left(S_t, t\right) dt + \sigma\left(S_t, t\right) dW_t, \qquad 0 \leq t < T, \tag{1.1}$$

where $\{W_t\}_t$ is Brownian motion process. The first term on the right-hand-side of (1.1)is deterministic(real-valued) and the second is diffusion(real-valued). Especially, in the context of option pricing, they are often called drift term and volatility term, respectively. T is time to option maturity. We want to calculate $E\left[P\left(S_T\right)\right]$,which is the expectation of discounted scalar payoff function value $P\left(S_T\right)$ for option pricing where P has a uniform Lipschitz bound; that is, there exists a constant c such that $\mid P(U) - P(V) \mid \leq c \parallel U - V \parallel$ for all U, V. To compute $E\left[P\left(S_T\right)\right]$, we need to discretize $\{S_t\}_t$. If we divide a time interval $[0, T]$ into $D \in \mathbb{N}$ subintervals $[0 = t_0 < t_1 < t_2 < \cdots < t_n < \cdots < t_D = T]$by setting a time step interval $\Delta t \equiv t_n - t_{n-1} = T/D$ for $n = 1, 2, \ldots, D$, the corresponding Euler scheme discretization of $\{S_t\}_t$ with Δt is given by

$$\widehat{S}_{t_{n+1}} - \widehat{S}_{t_n} = \mu\left(\widehat{S}_{t_n}, t_n\right) \Delta t + \sigma\left(\widehat{S}_{t_n}, t_n\right) \Delta W_{t_n}, n = 0, 1, \ldots, D-1. \tag{1.2}$$

where ΔW_{t_n} is a Brownian increment. We can compute $\widehat{Y}$ as $E\left[P\left(S_T\right)\right]$

$$\widehat{Y} = N^{-1} \sum_{i=1}^{N} P\left(\widehat{S}_T^{(i)}\right),$$

where N is the number of simulation paths. This is a standard Monte Carlo (SMC) method and $\widehat{Y}$ is the SMC estimator. Set $D = M^L$. Let $\widehat{P}_\ell, \ell = 0, 1, \ldots, L$ denote the approximation of $P(S_T)$ on level ℓ; $\widehat{P}_\ell$ is the discretized version of $P(S_T)$with a time step interval $h_\ell = T/M^\ell$. Under the MLMC framework, the expected value $E\left[\widehat{P}_L\right]$ on the finest level L can be uniquely constructed by

$$\mathrm{E}[\widehat{P}_L] = \mathrm{E}[\widehat{P}_0] + \sum_{\ell=1}^{L} \mathrm{E}[\widehat{P}_\ell - \widehat{P}_{\ell-1}] \tag{1.3}$$

Let $\widehat{Y}_0$ denote the estimator of $E\left[P_0\right]$ using N_0 simulation paths and let $\widehat{Y}_\ell, \ell = 1, 2, \ldots, L$ denote the estimators of $E\left[\widehat{P}_\ell - \widehat{P}_{\ell-1}\right], \ell = 1, 2, \ldots, L$ using N_ℓ simulation paths. Then, the MLMC estimator is constructed by

$$\widehat{Y} = \sum_{\ell=0}^{L} \widehat{Y}_\ell,$$

where

$$\widehat{Y}_\ell = \begin{cases} N_0^{-1} \sum_{i=1}^{N_0} \widehat{P}_0^i, & (\ell = 0), \\ N_\ell^{-1} \sum_{i=1}^{N_\ell} \left(\widehat{P}_\ell^i - \widehat{P}_{\ell-1}^i\right), & (0 < \ell \leq L). \end{cases}$$

Thus, we can consider the MLMC method as a Monte Carlo framework using an Euler scheme for pricing European style options that have Lipschitz payoff. However, Giles[2] reported that the MLMC method using the Euler scheme has numerically good performance for not only Lipschitz payoffs but also non Lipschitz payoffs. Giles[3] tested European vanilla options pricing under a scalar SDE and Heston model, and three Exotic

options(Asian, Lookback, and Digital options) pricing under a scalar SDE by the MLMC method using the Euler scheme. Furthermore, Giles, Higham, and Mao [5] mathematically analyzed non-Lipschitz payoffs based on the assumption of a global Lipschitz bounds that drift and diffusion coefficients of (1.1) satisfy, and reported that the MLMC using the Euler scheme can be mathematically justified for non-globally Lipschitz payoffs. In addition, the Milstein scheme, which is a higher order scheme compared to the Euler scheme (see Kloeden and Platen[12]), was applied to the MLMC method (see Giles[2], Giles, Debrabant, and Rößler[8]). Giles, Debrabant, and Rößler[8] mathematically analyzed the efficiency of the MLMC method using the Milstein scheme for pricing vanilla options and four exotic options (Asian, Lookback, Digital, and Barrier options) under scalar SDEs. Giles[2] offers numerical results of the MLMC method using the Milstein scheme for pricing four exotic options under a scalar SDE; Giles[2] reported that the MLMC method using the Milstein scheme is more efficient than the SMC method in computational cost reduction and that it improves multilevel convergence. There still is a higher order convergence scheme known as the order 1.5 Taylor strong scheme (see Kloeden and Platen [12]). However, there has been no study that tried to test the MLMC method using the order 1.5 Taylor strong scheme in our recognition. One direction of study is to test the numerical performance of the MLMC method using the order 1.5 Taylor strong scheme and another is a theoretical analysis of the method. In this study, we concentrate on the former. Note that in the MLMC method using the Milstein scheme, the Milstein scheme version of the former was researched by Giles[2] and the Milstein scheme version of the latter was studied by Giles, Debrabant, and Rößler[8]. In addition, other well-known exotic options and a very well-known stochastic volatility model have not been tested by the MLMC method using the Euler and the Milstein scheme, such as Power options, Rainbow options, Cliquet options, Exchange options, and the SABR model, which is used in many financial institutions. Such options and the SABR model should be tested under the MLMC framework.

This paper is organized as follows. In Section 2, we introduce the complexity theorem of the MLMC method of Giles [2]. Next, we introduce the Milstein scheme and the order 1.5 Taylor strong scheme. We then summarize the calculation of eight types of options payoff. Furthermore, we summarize the numerical results of the MLMC method using the Euler and the Milstein scheme in previous studies in the order of variance convergence of Y_ℓ. In Section 3, we demonstrate the numerical performance of the MLMC method using the order 1.5 Taylor strong scheme for eight different options pricing and using the Euler scheme based on the SABR model in computational complexity reduction and order of convergence. Finally, we summarize the numerical results in this paper and discuss a possible direction of future research.

2. The Complexity Theorem of Multilevel Monte Carlo method and Numerical Discretization Schemes of SDE

2.1. The Complexity Theorem

As noted in Section 1, the SMC method uses only one type of time step interval Δt to generate simulation paths; however, the MLMC method uses multiple types of time step intervals $h_\ell = T/M^\ell, 0 \leq \ell \leq L$ to generate simulation paths. Then the MLMC estimator$\widehat{Y}$ is estimated by paths generated by time steps $h_\ell, 0 \leq \ell \leq L$. The following theorem of the MLMC method was proven by Giles[3]. The theorem gives a bound of computational cost for the MLMC estimator $\widehat{Y}$ to attain the required accuracy.

Theorem 2.1 (Giles[3]). *Let P denote a function of the solution of SDE (1.1) for a given*

Brownian path $W(t)$, and, let $\widehat{P}_\ell$ denote the corresponding level ℓ of numerical approximation using a numerical discretization with time step $h_\ell = M^{-\ell}T$.

If there exist independent estimators $\widehat{Y}_\ell$ based on N_ℓ Monte Carlo samples, and positive constants $\alpha \geq \frac{1}{2}, \beta, \gamma, c_1, c_2, c_3$ such that

i) $|E[\widehat{P}_\ell - P]| \leq c_1 h_\ell^\alpha$,

ii) $E[\widehat{Y}_\ell] = \begin{cases} E[\widehat{P}_0], & \ell = 0, \\ E[\widehat{P}_\ell - \widehat{P}_{\ell-1}], & \ell > 0, \end{cases}$

iii) $V[\widehat{Y}_\ell] \leq c_2 N_\ell{}^{-1} h_\ell^\beta$,

iv) C_ℓ, *the computational complexity of* $\widehat{Y}_\ell$, *is bounded by*

$$C_\ell \leq c_3 N_\ell h_\ell^{-1},$$

then, there exists a positive constant c_4 such that for any $\epsilon < e^{-1}$ there are values L and N_ℓ for which the multilevel estimator

$$\widehat{Y} = \sum_{\ell=0}^{L} \widehat{Y}_\ell,$$

has a mean-square-error with bound

$$MSE \equiv E\left[\left(\widehat{Y} - E[P]\right)^2\right] < \epsilon^2$$

with a computational complexity C with bound

$$C \leq \begin{cases} c_4 \epsilon^{-2}, & \beta > 1, \\ c_4 \epsilon^{-2} (\log \epsilon)^2, & \beta = 1, \\ c_4 \epsilon^{-2-(\gamma-\beta)/\alpha}, & 0 < \beta < 1. \end{cases}$$

Proof. See Giles [3]. □

Note that the SMC method requires the computational complexity $O(\epsilon^{-3})$ to make the MSE $O(\epsilon^2)$. The complexity theorem claims that the MLMC estimator $\widehat{Y}$ can achieve the required accuracy, MSE $< \epsilon^2$, with less computational complexity than the SMC method. In addition, note that the MSE can be represented as follows.

$$\begin{aligned} \text{MSE} &= \text{E}[(\widehat{Y} - \text{E}[P])^2] \\ &= \text{E}[(\widehat{Y} - \text{E}[\widehat{Y}])^2] + (\text{E}[\widehat{Y}] - \text{E}[P])^2 \end{aligned} \tag{2.1}$$

where the first term on the right-hand side in (2.1), $\text{E}[(\widehat{Y} - \text{E}[\widehat{Y}])^2]$, is the variance of the estimator and the second term, $(\text{E}[\widehat{Y}] - \text{E}[P])^2$, is the square of its bias due to discrete approximation. The MLMC method reduces the first term and the variance reduction effect leads to reduction in computational complexity.

2.2. Two Higher Order Discretization Schemes: The Milstein scheme and the Order 1.5 Taylor Strong scheme

Let $a_t \equiv \mu\left(\widehat{S}_t, t\right)$ and $b_t \equiv \sigma\left(\widehat{S}_t, t\right)$ for all $0 < t < T$. The Milstein discretization of SDE (1.1) is given by

$$\begin{aligned} &\widehat{S}_{t_{n+1}} - \widehat{S}_{t_n} = a_{t_n}\Delta t + b_{t_n}\Delta W_{t_n} + \frac{1}{2} b'_{t_n} b_{t_n} (\Delta W_{t_n}^2 - \Delta t), \\ &n = 0, 1, \ldots, D-1 \end{aligned} \tag{2.2}$$

where $b'_{t_n} = \partial b_{t_n}/\partial S_{t_n}$. The Milstein scheme increases the approximation accuracy of the SDE by adding a second-order term to the Euler scheme in (1.2). The strong and weak orders of convergence in the Euler scheme are equal to 0.5 and 1, respectively; however, both strong and weak orders of convergence of the Milstein scheme are equal to 1. Giles [2] numerically tests the MLMC method using a Milstein scheme. In addition, Giles, Debrabant, and Rößler [8] mathematically analyze the method in the variance of the multilevel estimator. The latter paper assumes that the drift function and the volatility function of (1.1) satisfy certain standard conditions that are uniform Lipschitz conditions, a linear growth bound, and an additional Lipschitz condition (see section 2.1 in Giles, Debrabant, and Rößler [8]). Our interest is the numerical performance of the MLMC method using the order 1.5 Taylor strong scheme. However, in a mathematical analysis of MLMC method using the order 1.5 Taylor strong scheme we should discuss theoretical analysis on the basis of Theorem 10.6.3 in Kloeden and Platon [12], as it gives the conditions under which the order 1.5 Taylor strong scheme actually attains the order 1.5 of strong convergence. The order 1.5 Taylor strong scheme increases accuracy by adding more terms to the Milstein scheme (2.2). Thus, order 1.5 Taylor discretization of SDE (1.1) is given by

$$\begin{aligned}\widehat{S}_{t_{n+1}} - \widehat{S}_{t_n} =& a_{t_n}\Delta t + b_{t_n}\Delta W_{t_n} + \frac{1}{2}b'_{t_n}b_{t_n}(\Delta W_{t_n}^2 - \Delta t) + \\ & \frac{1}{2}a_{t_n}a'_{t_n}\Delta t^2 + a_{t_n}b'_{t_n}\Delta t\Delta W_{t_n} + \\ & \frac{1}{2}b_{t_n}(b'_{t_n})^2(\frac{1}{3}\Delta W_{t_n}^2 - \Delta t)\Delta W_{t_n}, \quad n = 0, 1, \ldots, D-1 \end{aligned} \tag{2.3}$$

where $a'_{t_n} = \partial a_{t_n}/\partial S_{t_n}$ and $b'_{t_n} = \partial b_{t_n}/\partial S_{t_n}$.

2.3. Numerical Results in Previous Works using Euler and Milstein Schemes

If level $\ell > 0$ is fine level, level $\ell - 1$ is coarse level. We denote $\widehat{P}_\ell^f \equiv \widehat{P}_\ell$ and $\widehat{P}_{\ell-1}^c \equiv \widehat{P}_{\ell-1}$. If level ℓ is equal to 0, level $\ell - 1$ does not exist. We denote $\widehat{P}_\ell^f \equiv \widehat{P}_\ell$. If level $\ell + 1$ is fine level, level ℓ is coarse level. We denote $\widehat{P}_{\ell+1}^f \equiv \widehat{P}_{\ell+1}$ and $\widehat{P}_\ell^c \equiv \widehat{P}_\ell$. Giles[2] explained that the following equation is required to secure (1.3):

$$E[\widehat{P}_\ell^f] = E[\widehat{P}_\ell^c], \quad 0 \le \ell \le L - 1. \tag{2.4}$$

Numerical results in Giles [2]·[3] in Table 1 were for a geometric Brownian motion with constants r and v

$$dS_t = rSdt + vS_t dW_t, \quad 0 \le t < T. \tag{2.5}$$

Table 1 shows the numerical order of variance convergence of Y_ℓ with the MLMC method using the Euler and the Milstein scheme in Giles[2][3] .

	Euler scheme	Milstein scheme
Vanilla option	$\mathcal{O}(h)$	-
Asian option	$\mathcal{O}(h)$	$\mathcal{O}(h^2)$
Lookback option	$\mathcal{O}(h)$	$\mathcal{O}(h^2)$
Digital option	$\mathcal{O}(h^{1/2})$	$\mathcal{O}(h^{3/2})$
Barrier option	-	$\mathcal{O}(h^{3/2})$

M in the complexity theorem was set to be 4 in Giles[3]. However, M was set to be 2 in Giles[2]. Although the two papers treat the same types of Exotic options as follows:

Asian option, Lookback option, and Digital option, their method of calculating payoff is different. Giles[2] uses Brownian interpolation results based on Glasserman[9]. The results are presented in section 3 of Giles [2] and section 2,3 of Giles [8], and the aim is to achieve an improved convergence rate using the Milstein scheme and to satisfy (2.4) (see section 3.1, 3.3, and 3.5 in Giles[2]). In this study the three exotic options pricing of the MLMC method using the order 1.5 Taylor strong scheme is based on Giles[2],[8] .

In the MLMC method, $\widehat{Y}_\ell$ is the estimator of $E\left[\widehat{P}_\ell - \widehat{P}_{\ell-1}\right] \equiv E\left[\widehat{P}_\ell^f - \widehat{P}_{\ell-1}^c\right]$ is calculated by using both fine level ℓ and coarse level $\ell-1$ simulation paths. $E\left[\widehat{P}_\ell^f - \widehat{P}_{\ell-1}^c\right]$ is the expectation of the difference between fine level discounted payoff and coarse level discounted payoff. If M is equal to 4, fine level L simulation paths, which are generated by using the discretization of (2.5) with time step h_L, are $\{\widehat{S}_{t_0}^{f,i}, \widehat{S}_{t_1}^{f,i}, \widehat{S}_{t_2}^{f,i}, \ldots, \widehat{S}_{t_D}^{f,i}\}, i = 1, 2, \ldots, N_L$, and coarse level $L-1$ simulation paths, which are generated by using the discretization of (2.5) with time step h_{L-1}, are $\{\widehat{S}_{t_0}^{c,i}, \widehat{S}_{t_4}^{c,i}, \widehat{S}_{t_8}^{c,i}, \ldots, \widehat{S}_{t_D}^{c,i}\}, i = 1, 2, \ldots, N_L$. Then we denote $\{\widehat{S}_{t_n}^{f,i}\}_{n=0,1,\ldots,D}, \{\widehat{S}_{t_n}^{c,i}\}_{n=0,4,\ldots,D}$ as $\{\dot{S}_m^{f,i}\}_{m=0,1,\ldots,4^L}, \{\dot{S}_m^{c,i}\}_{m=0,1,\ldots,4^{L-1}}$. If M is equal to 2, fine level ℓ simulation paths are $\{\widehat{S}_{t_0}^{f,i}, \widehat{S}_{t_1}^{f,i}, \widehat{S}_{t_2}^{f,i}, \ldots, \widehat{S}_{t_D}^{f,i}\}, i = 1, 2, \ldots, N_L$, and coarse level $L-1$ simulation paths are $\{\widehat{S}_{t_0}^{c,i}, \widehat{S}_{t_2}^{c,i}, \widehat{S}_{t_4}^{c,i}, \ldots, \widehat{S}_{t_D}^{c,i}\}, i = 1, 2, \ldots, N_L$. If $L-1$ is fine level, fine level $L-1$ and coarse level $L-2$ simulation paths are $\{\widehat{S}_{t_0}^{f,i}, \widehat{S}_{t_2}^{f,i}, \widehat{S}_{t_4}^{f,i}, \ldots, \widehat{S}_{t_D}^{f,i}\}, i = 1, 2, \ldots, N_{L-1}$ and $\{\widehat{S}_{t_0}^{c,i}, \widehat{S}_{t_4}^{c,i}, \widehat{S}_{t_8}^{c,i}, \ldots, \widehat{S}_{t_D}^{c,i}\}, i = 1, 2, \ldots, N_{L-1}$, respectively. Then we denote $\{\widehat{S}_{t_n}^{f,i}\}_{n=0,2,\ldots,D}, \{\widehat{S}_{t_n}^{c,i}\}_{n=0,4,\ldots,D}$ as $\{\dot{S}_m^{f,i}\}_{m=0,1,\ldots,2^{L-1}}, \{\dot{S}_m^{c,i}\}_{m=0,1,\ldots,2^{L-2}}$. The following two subsections summarize how to price each option, based on (2.5), in the Euler scheme case (Giles [3]) and the Milstein scheme case (Giles [2],[8]). F is each option payoff. The fine level payoff $\widehat{P}_\ell^{f,i}$ and the coarse level payoff $\widehat{P}_{\ell-1}^{c,i}$ are calculated as follows.

2.3.1. Euler Scheme Case (Giles [3])

- European vanilla call option

$$
\begin{aligned}
F &= \exp(-rT)\max(0, S_T - K).\\
\widehat{P}_\ell^{f,i} &= \exp(-rT)\max(0, \widehat{S}_D^{f,i} - K), \quad i = 1, 2, \ldots, N_\ell,\\
\widehat{P}_{\ell-1}^{c,i} &= \exp(-rT)\max(0, \widehat{S}_D^{c,i} - K), \quad i = 1, 2, \ldots, N_\ell.
\end{aligned}
$$

- Asian call option

$$F = \exp(-rT)\max(0, \overline{S} - K),$$

where the mean value over the time interval is defined by

$$
\begin{aligned}
\overline{S} &\equiv T^{-1}\int_0^T S_t dt.\\
\widehat{P}_\ell^{f,i} &= \exp(-rT)\max(0, \overline{\widehat{S}}_\ell^{f,i} - K), \quad i = 1, 2, \ldots, N_\ell,\\
\widehat{P}_{\ell-1}^{c,i} &= \exp(-rT)\max(0, \overline{\widehat{S}}_{\ell-1}^{c,i} - K), \quad i = 1, 2, \ldots, N_\ell.
\end{aligned}
$$

where the mean value are expressed as follows.

$$
\begin{aligned}
\overline{\widehat{S}}_\ell^{f,i} &= T^{-1}\sum_{m=0,1,\ldots,M^\ell-1}\frac{1}{2}(\dot{S}_m^{f,i} + \dot{S}_{m+1}^{f,i})h_\ell, \quad i = 1, 2, \ldots, N_\ell,\\
\overline{\widehat{S}}_{\ell-1}^{c,i} &= T^{-1}\sum_{m=0,1,\ldots,M^{\ell-1}-1}\frac{1}{2}(\dot{S}_m^{c,i} + \dot{S}_{m+1}^{c,i})h_{\ell-1}, \quad i = 1, 2, \ldots, N_\ell.
\end{aligned}
$$

- Lookback call option

$$
\begin{aligned}
F &= \exp(-rT)\left(S_T - \min_{0\le t<T} S_t\right).\\
\widehat{P}_\ell^{f,i} &= \exp(-rT)\left(\widehat{S}_{t_D}^{f,i} - \widehat{S}_{\min,\ell}^{f,i}\right), \quad i = 1,2,\ldots,N_\ell,\\
\widehat{P}_{\ell-1}^{c,i} &= \exp(-rT)\left(\widehat{S}_{t_D}^{c,i} - \widehat{S}_{\min,\ell-1}^{c,i}\right), \quad i = 1,2,\ldots,N_\ell.
\end{aligned}
$$

where the minimum value of S_t over the path is calculated by

$$
\begin{aligned}
\widehat{S}_{\min,\ell}^{f,i} &= \left(\min_{m=0,1,\ldots,M^\ell} \dot{S}_m^{f,i}\right)\left(1 - \beta^* v\sqrt{h_\ell}\right), \quad i = 1,2,\ldots,N_\ell,\\
\widehat{S}_{\min,\ell-1}^{c,i} &= \left(\min_{m=0,1,,\ldots,M^{\ell-1}} \dot{S}_m^{c,i}\right)\left(1 - \beta^* v\sqrt{h_{\ell-1}}\right), \quad i = 1,2,\ldots,N_\ell,
\end{aligned}
$$

with $\beta^* \approx 0.5826$.

- Digital call option

$$
\begin{aligned}
F &= \exp(-rT)H\left(S_T - K\right).\\
\widehat{P}_\ell^{f,i} &= \exp(-rT)H\left(\widehat{S}_{t_D}^{f,i} - K\right), i = 1,2,\ldots,N_\ell,\\
\widehat{P}_\ell^{c,i} &= \exp(-rT)H\left(\widehat{S}_{t_D}^{c,i} - K\right), i = 1,2,\ldots,N_\ell,
\end{aligned}
$$

where $H(x)$ is the Heaviside function.

2.3.2. Milstein Scheme Case (Giles [2], [8])

- Asian option

$$
\begin{aligned}
F &= \exp(-r)\max(0, \overline{S} - K).\\
\widehat{P}_\ell^{f,i} &= \exp(-rT)\max(0, \overline{\widehat{S}}_\ell^{f,i} - K), \quad i = 1,2,\ldots,N_\ell,\\
\widehat{P}_{\ell-1}^{c,i} &= \exp(-rT)\max(0, \overline{\widehat{S}}_{\ell-1}^{c,i} - K), \quad i = 1,2,\ldots,N_\ell.\\
\overline{\widehat{S}}_\ell^{f,i} &= T^{-1}\sum_{m=0,1,\ldots,M^\ell-1}\left(\frac{1}{2}(\dot{S}_m^{f,i} + \dot{S}_{m+1}^{f,i})h_\ell + \Delta I_m^{f,i}\right), \quad i = 1,2,\ldots,N_\ell,\\
\overline{\widehat{S}}_{\ell-1}^{c,i} &= T^{-1}\sum_{m=0,1,\ldots,M^{\ell-1}-1}\left(\frac{1}{2}(\dot{S}_m^{c,i} + \dot{S}_{m+1}^{c,i})h_{\ell-1} + \Delta I_m^{c,i}\right), \quad i = 1,2,\ldots,N_\ell,
\end{aligned}
$$

where $\Delta I_m^{f,i}$ is a $N(0, h_\ell^3/12)$ random variable. $\Delta I_m^{c,i}$ is calculated by

$$
\Delta I_m^{c,i} = \Delta I_m^{f,i} + \Delta I_{m+1}^{f,i} + \frac{1}{2}h_\ell(\Delta W_m - \Delta W_{m+1}).
$$

Note that $\Delta I_m^{f,i}$, $\Delta I_{m+1}^{f,i}, \Delta W_m$, and ΔW_{m+1} come from corresponding fine path simulation.

- Lookback option

$$
\begin{aligned}
F &= \exp(-rT)\left(S_T - \min_{0\le t\le T} S_t\right),\\
\widehat{P}_\ell^{f,i} &= \exp(-rT)\left(\widehat{S}_{t_D}^{f,i} - \widehat{S}_{\min,\ell}^{f,i}\right), \quad i = 1,2,\ldots,N_\ell,\\
\widehat{P}_{\ell-1}^{c,i} &= \exp(-rT)\left(\widehat{S}_{t_D}^{c,i} - \widehat{S}_{\min,\ell-1}^{c,i}\right), \quad i = 1,2,\ldots,N_\ell.
\end{aligned}
$$

Then the minimum value of S_t over the path is calculated by

$$\widehat{S}^{f,i}_{\min,\ell} = \min_{0\le m\le M^\ell-1} \dot{S}^{f,i}_{m,\min,\ell},$$
$$\widehat{S}^{c,i}_{\min,\ell-1} = \min_{0\le m\le M^{\ell-1}-1} \dot{S}^{c,i}_{m,\min,\ell-1},$$

where

$$\widehat{S}^{f,i}_{m,\min,\ell} = \frac{1}{2}\left(\dot{S}^{f,i}_m + \dot{S}^{f,i}_{m+1} - \sqrt{(\dot{S}^{f,i}_{m+1} - \dot{S}^{f,i}_m)^2 - 2v^2 h \log U^i_m}\right),$$
$$\widehat{S}^{c,i}_{m,\min,\ell-1} = \min\left(x1, x2\right).$$

Here $x1$ and $x2$ are

$$x1 = \frac{1}{2}\left(\dot{S}^{c,i}_m + \dot{S}^{c,i}_{m+1} - \sqrt{(\dot{S}^{c,i}_{m+1} - \dot{S}^{c,i}_m)^2 - 2v^2 h_\ell \log U^i_m}\right),$$
$$x2 = \frac{1}{2}\left(\dot{S}^{c,i}_{m+1} + \dot{S}^{c,i}_{m+2} - \sqrt{(\dot{S}^{c,i}_{m+2} - \dot{S}^{c,i}_{m+1})^2 - 2v^2 h_\ell \log U^i_{m+1}}\right).$$

Then U^i_m and U^i_{m+1} from the simulation of $\widehat{P}^{f,i}_\ell$ are uniform random variables, and the Brownian interpolation value $\dot{S}^{c,i}_{m+1}$ is calculated by

$$\dot{S}^{c,i}_{m+1} = \frac{1}{2}(\dot{S}^{f,i}_m + \dot{S}^{f,i}_{m+1} - vD^i_m),$$

where

$$D^i_m = (W^i_{m+2} - W^i_{m+1}) - (W^i_{m+1} - W^i_m)$$

is a $N(0, h_\ell)$ random variable.

- Digital option

$$F = \exp(-rT)1_{\{S_T>K\}}(S_T),$$

where $1_{\{S_T>K\}}$ is an indicator function. Note that $1_{\{S_T>K\}}(S_T)$ coincides with $H(S_T - K)$ in subsection 2.3.1.

$$\widehat{P}^{f,i}_\ell = \exp(-rT)\widehat{p}^{f,i,\ell},$$
$$\widehat{P}^{c,i}_{\ell-1} = \exp(-rT)\widehat{p}^{c,i,,\ell-1},$$

where

$$\widehat{p}^{f,i,\ell} = \Phi\left(\frac{\dot{S}^{f,i}_{M^\ell-1} + rh_\ell - K}{|v|\sqrt{h_\ell}}\right),$$
$$\widehat{p}^{c,i,,\ell-1} = \Phi\left(\frac{\dot{S}^{c,i}_{M^{\ell-1}-1} + 2rh_\ell + v\Delta W^i_{M^{\ell-1}-1} - K}{|v|\sqrt{h_\ell}}\right).$$

Here $\Phi(\cdot)$ is the cumlative normal distribution function.

3. Numerical Results

All numerical results are based on the results of Giles [2]'Giles [3] . Thus the verification contents are the convergence of both V_ℓ and $E[\widehat{P}_\ell - \widehat{P}_{\ell-1}]$ and the effect of computational complexity reduction. Each result, except for subsection 3.2.2, 3.2.4, and 3.3 is presented for the SDE (2.5). We set $S_0 = 1$, $r = 0.05$, $v = 0.2$, $T = 1$, and strike price $K = 1$. In each payoff case, except subsection 3.3, we set $M = 2$. In subsection 3.3, we set $M = 4$. In addition, The estimated quantities of the top plots of all odd-numbered figures, Figure 18, and Figure 20 are based on 10^7 simulation paths. Here we refer to the MLMC method using the Euler scheme, the Milstein scheme, and the order 1.5 Taylor strong scheme as "MLMC (Elr)," "MLMC (Mls)," and "MLMC (Tlr)," respectively. As with the MLMC (Elr), the MLMC (Mls), and the MLMC (Tlr), we use "SMC (Elr)," "SMC (Mls)," and "SMC (Tlr)."

3.1. Performance of MLMC method using Order 1.5 Taylor strong scheme

We verify whether the MLMC (Tlr) is numerically superior to the SMC (Tlr) in the valuation of four options (European vanilla, Asian, Lookback, and Digital). We also numerically compare the performance of the MLMC (Tlr) and the performance of the MLMC (Elr) as a reference. Note that Giles [3] tested the four options using the MLMC (Elr) with $M = 4$. The top left plot of Figure 1, 3, 5, and 7 shows the convergence of V_ℓ, and the top right plot shows the convergence of $E[\widehat{P}_\ell - \widehat{P}_{\ell-1}]$: The top left plot's slope of $-x(x > 0)$ and the top right plot's slope of $-y(y > 0)$ mean that $V(h_\ell) = O(h_\ell^x)$ and $E[\widehat{P}_\ell - \widehat{P}_{\ell-1}] = O(h_\ell^y)$. The bottom left plot offers a comparison of computational cost between the MLMC (Tlr) and the MLMC (Elr). The two left plots of Figure 2, 4, 6, and 8 show the number of simulation paths for the MLMC (Elr) or the MLMC (Tlr) to achieve an accuracy ϵ for five different values of ϵ. The two right plots show the total computational cost for them to attain an accuracy ϵ for five different values of ϵ. Note that the MLMC method using the Euler scheme and the calculations of subsection 2.3.2 based on the Brownian interpolation method, the "MLMC (EBM)," can achieve a significant reduction in computational cost, compared to the MLMC (Elr) (see Figure 18-20).

3.1.1. European vanilla option

As with $M = 4$ in Giles [3], in the MLMC (Elr) with $M = 2$, the two top plots of Figure 1 show that $V_\ell = O(h_\ell)$ and $E[\widehat{P}_\ell - \widehat{P}_{\ell-1}] = O(h_\ell)$. Furthermore, they show that the MLMC (Tlr) has faster convergence than the MLMC (Elr). The MLMC (Tlr)'s slope of -3 means a $O(h_\ell^3)$ convergence of V_ℓ. At $\ell = 2, 3$ a line of $E[\widehat{P}_\ell - \widehat{P}_{\ell-1}]$ for the MLMC (Tlr) shows faster weak convergence. For $l = 4$, V_ℓ of the MLMC (Tlr) is more than 10,000,000 times smaller than $V[\widehat{P}_\ell]$ of both the SMC (Tlr) and the SMC (Elr), and is more than 10,000 times smaller than V_ℓ of the MLMC (Elr). Compared with the SMC (Tlr), the bottom right plot of Figure 2 shows that the MLMC (Tlr) attains computational cost reduction of more than 90%. Compared with the MLMC (Elr), the MLMC (Tlr) attains a computational cost reduction of about 70-80%.

3.1.2. Asian option

The top left plot of Figure 3 shows the MLMC (Tlr)'s slope of -3. It means the $O(h_\ell^3)$ convergence of V_ℓ. The top right plot of Figure 3 shows the MLMC (Tlr)'s slope of -3. It means the $O(h_\ell)$ convergence of $E[\widehat{P}_\ell - \widehat{P}_{\ell-1}]$. Compared with the SMC (Tlr), the bottom right plot of Figure 4 shows that MLMC (Tlr) attains a computational complexity reduction of more than 90%. As with the results with $M = 4$ in Giles [3], in the case of the MLMC (Elr) with $M = 2$, the two top plots of Figure 3 show $O(h_\ell)$ convergence of V_ℓ and $E[\widehat{P}_\ell - \widehat{P}_{\ell-1}]$. The top left plot of Figure 3 shows that the MLMC (Tlr) has faster strong convergence than

the MLMC (Elr); however, the top right plot of Figure 3 shows that the MLMC (Tlr) and the MLMC (Elr) have the same order of weak convergence. V_ℓ of the MLMC (Tlr) is more than 10,000 times smaller than $V[\widehat{P}_\ell]$ of both the SMC (Tlr) and the SMC (Elr) for $\ell = 3$, and is more than 1,000 times smaller than V_ℓ of the MLMC (Elr) for $\ell = 5$. Compared with the MLMC (Elr), the bottom left plot of Figure 4 shows that the MLMC (Tlr) attains a computational cost reduction of about 85-90%.

3.1.3. Lookback option

The top left plot of Figure 5 shows the MLMC (Tlr)'s slope of -3. It means the $O(h_\ell^3)$ convergence of V_ℓ. As in the Asian option case, the top right plot shows the MLMC (Tlr)'s slope of -3. It means the $O(h_\ell)$ convergence of $E[\widehat{P}_\ell - \widehat{P}_{\ell-1}]$. Compared with the SMC (Tlr), the bottom right plot of Figure 6 shows that the MLMC (Tlr) attains a computational cost reduction of more than 99%. As with the results of $M = 4$ in Giles [3], in the case of the MLMC (Elr) with $M = 2$, the two top plots of Figure 5 show approximately $O(h_\ell)$ convergence of V_ℓ and $E[\widehat{P}_\ell - \widehat{P}_{\ell-1}]$. As in the Asian option case, the top left plot of Figure 5 shows that the MLMC (Tlr) has faster strong convergence than the MLMC (Elr); however, the top right plot shows that the MLMC (Tlr) and the MLMC (Elr) have the same order of weak convergence. For $l = 5$, the V_ℓ of the MLMC (Tlr) is more than 10,000 times smaller than $V[\widehat{P}_\ell]$ of both the SMC (Tlr) and the SMC (Elr), and is more than 100 times smaller than the V_ℓ of the MLMC (Elr). For $l = 8$, the V_ℓ of the MLMC (Tlr) is more than 1,000,000 times smaller than $V[\widehat{P}_\ell]$ of both the SMC (Tlr) and the SMC (Elr), and is more than 1,000 times smaller than the V_ℓ of the MLMC (Elr). Compared with the MLMC (Elr), the bottom left plot of Figure 5 shows that the MLMC (Tlr) attains a computational cost reduction of approximately 95% for $\epsilon = 5.0 \times 10^{-5}$.

3.1.4. Digital option

As with the results of $M = 4$ in Giles [3], in the case of the MLMC (Elr) with $M = 2$, the two top plots of Figure 7 show that $V_\ell = O(h_\ell^{1/2})$ and $E[\widehat{P}_\ell - \widehat{P}_{\ell-1}] = O(h_\ell)$. In addition, they show that the MLMC (Tlr) has faster strong and weak convergence than the MLMC (Elr). The MLMC (Tlr)'s slope of $-3/2$ means the $O(h_\ell^{3/2})$ convergence of V_ℓ. The MLMC (Tlr)'s slope of -2 means the $O(h_\ell^2)$ convergence of $E[\widehat{P}_\ell - \widehat{P}_{\ell-1}]$. For $l = 6$, the V_ℓ of the MLMC (Tlr) is more than 10,000 times smaller than the $V[\widehat{P}_\ell]$ of both the SMC (Tlr) and the SMC (Elr), and is more than 500 times smaller than the V_ℓ of the MLMC (Elr). Compared with the SMC (Tlr), the bottom right plot of Figure 8 shows that the MLMC (Tlr) attains a computational cost reduction of up to 99.9%. Compared with the MLMC (Elr), the bottom left plot of Figure 7 shows that the MLMC (Tlr) attains a computational cost reduction of up to 99.9%.

3.2. Comparison of MLMC methods using Three Discretization schemes

We compare the performance between the MLMC (Elr), the MLMC (Mls), and the MLMC (Tlr) for pricing the other four exotic options (Power, Rainbow, Cliquet, and Exchange). The four options have not been tested by the MLMC method in previous studies. The top left plot of Figure 9, 11, 13, and 15 shows the convergence of V_ℓ. The top right plot shows the convergence of $E[\widehat{P}_\ell - \widehat{P}_{\ell-1}]$. The three left plots of Figure 10, 12, 14, and 16 show the number of paths for the MLMC (Elr), or the MLMC (Mls), or the MLMC (Tlr) to achieve an accuracy ϵ for five different values of ϵ. The three right plots show the total computational cost for them to attain the accuracies. The bottom left plot offers a comparison of computational cost between the MLMC (Tlr), the MLMC (Mls), and the MLMC (Elr).

3.2.1. Power option

The Power call option discounted payoff is given by

$$F = \exp(-rT)\max\left(S_T^G - K^G, 0\right)$$

with constant $G > 0$. The fine level and the coarse level discounted payoffs are calculated by

$$\widehat{P}_\ell^{f,i} = \exp(-rT)\max(0, (\widehat{S}_{t_D}^{f,i})^G - K^G), \quad i = 1, 2, \ldots, N_\ell,$$
$$\widehat{P}_{\ell-1}^{c,i} = \exp(-rT)\max(0, (\widehat{S}_{t_D}^{c,i})^G - K^G), \quad i = 1, 2, \ldots, N_\ell.$$

We set $G = 2$. The two top plots in Figure 9 show that the MLMC (Tlr)'s convergence of both V_ℓ and $E[\widehat{P}_\ell - \widehat{P}_{\ell-1}]$, $O(h_\ell^3)$ and $O(h_\ell^2)$, is the fastest of the three. In addition, they show that the MLMC (Mls)'s convergence of $E[\widehat{P}_\ell - \widehat{P}_{\ell-1}]$, $O(h_\ell)$, is about the same as the MLMC (Elr) and that $V(h_\ell)$ convergence of the MLMC (Mls), $O(h_\ell^2)$, is faster than that of the MLMC (Elr), $O(h_\ell)$. The top left plot shows that the SMC (Tlr), the SMC (Mls), and the SMC (Elr) have about the same variance, $V[\widehat{P}_\ell]$. For $l = 3$, the V_ℓ of the MLMC (Tlr) is more than 1,000,000 times smaller than $V[\widehat{P}_\ell]$, and is more than 100 times smaller than the V_ℓ of the MLMC (Mls), and is more than 1,000 times smaller than the V_ℓ of the MLMC (Elr). Figure 10 shows the computational cost of MLMC and SMC. Compared with the SMC (Elr), the SMC (Mls), and the SMC (Tlr), the MLMC (Elr), the MLMC (Mls), and the MLMC (Tlr) significantly reduce computational cost, respectively. The two bottom plots of Figure 9 show that the MLMC (Tlr) needs smallest computational cost to achieve required accuracy ϵ. Compared with the MLMC (Mls), the MLMC (Tlr) attains a computational cost reduction of about 15% for five different values of ϵ.

3.2.2. Rainbow option

We treat two-color Rainbow call option. The discounted payoff is given by

$$F = \exp(-rT)\max\left(\max[S^1(T), S^2(T)] - K, 0\right)$$

where $\{S_t^1\}_t$ and $\{S_t^2\}_t$ are two geometric Brownian motions with constants r_1, r_2, v_1, and v_2

$$dS_t^1 = r_1 S_t^1 dt + v_1 S_t^1 dW_t^1, \qquad 0 \le t < T,$$
$$dS_t^2 = r_2 S_t^2 dt + v_2 S_t^2 dW_t^2, \qquad 0 \le t < T,$$

where $\{W_t^1\}_t$ and $\{W_t^2\}_t$ are correlated with $dW_t^1 dW_t^2 = \rho dt$ with $\rho \in [-1, 1]$. The fine and the coarse level discounted payoffs are calculated by

$$\widehat{P}_\ell^{f,i} = \exp(-rT)\max\left(\max[\widehat{S}_{t_D}^{1,f,i}, \widehat{S}_{t_D}^{2,f,i}] - K, 0\right), \quad i = 1, 2, \ldots, N_\ell,$$
$$\widehat{P}_{\ell-1}^{c,i} = \exp(-rT)\max\left(\max[\widehat{S}_{t_D}^{1,c,i}, \widehat{S}_{t_D}^{2,c,i}] - K, 0\right), \quad i = 1, 2, \ldots, N_\ell.$$

We set $S_0^1 = S_0^2 = 1$, $r_1 = r_2 = 0.05$, $v_1 = v_2 = 0.2$, and $\rho = 0.4$. The result denotes the same tendency as the Power option case. The two top plots of Figure 11 show that the MLMC (Tlr)'s convergence of both V_ℓ and $E[\widehat{P}_\ell - \widehat{P}_{\ell-1}]$, $O(h_\ell^3)$ and $O(h_\ell^2)$, is the fastest of the three. Further, they show that the MLMC (Mls)'s convergence of $E[\widehat{P}_\ell - \widehat{P}_{\ell-1}]$, $O(h_\ell)$, is about the same as the MLMC (Elr) and that $V(h_\ell)$ convergence of the MLMC (Mls), $O(h_\ell^2)$,

is faster than that of the MLMC (Elr), $O(h_\ell)$. The top left plot of Figure 11 shows that the three SMC methods have about the same variance, $V[\widehat{P}_\ell]$. For $l = 4$, the V_ℓ of the MLMC (Tlr) is about 1,000,000 times smaller than $V[\widehat{P}_\ell]$, and is more than 100 times smaller than the V_ℓ of the MLMC (Mls), and is more than 10,000 times smaller than the V_ℓ of the MLMC (Elr). Figure 12 shows the computational cost of MLMC and SMC. Compared with the SMC (Elr), the SMC (Mls), and the SMC (Tlr), the MLMC (Elr), the MLMC (Mls), and the MLMC (Tlr) significantly reduce computational cost, respectively. The two bottom plots of Figure 11 show that the MLMC (Tlr) needs smallest computational cost to achieve required accuracy ϵ. Compared with the MLMC (Mls), the MLMC (Tlr) attains a slight computational cost reduction of about 5-15%.

3.2.3. Cliquet option

We treat the Cliquet call option whose discounted payoff is given by

$$F_1 = \exp(-rT_1)\max\left(S_{T_1} - K, 0\right),$$
$$F_2 = \exp(-rT)\max\left(S_T - S_{T_1}, 0\right)$$

with $T_1 = T/2$. Note that we set the minimum level as 1, since we consider the semiannual payoff. The fine level and the coarse level discounted payoffs are calculated by

$$\widehat{P}_{1,\ell}^{f,i} = \exp(-rT_1)\max(0, \widehat{S}_{T_1}^{f,i} - K), \quad i = 1, 2, \ldots, N_\ell,$$
$$\widehat{P}_{1,\ell-1}^{c,i} = \exp(-rT_1)\max(0, (\widehat{S}_{T_1}^{c,i} - K), \quad i = 1, 2, \ldots, N_\ell,$$
$$\widehat{P}_{2,\ell}^{f,i} = \exp(-rT)\max(0, \widehat{S}_{t_D}^{f,i} - K), \quad i = 1, 2, \ldots, N_\ell,$$
$$\widehat{P}_{2,\ell-1}^{c,i} = \exp(-rT)\max(0, \widehat{S}_{t_D}^{c,i} - K), \quad i = 1, 2, \ldots, N_\ell.$$

The result except $E[\widehat{P}_\ell - \widehat{P}_{\ell-1}]$ convergence has the same tendency in both the Power option and Rainbow option results. The two top plots of Figure 13 show that the MLMC (Tlr)'s convergence of both V_ℓ and $E[\widehat{P}_\ell - \widehat{P}_{\ell-1}]$, $O(h_\ell^3)$ and $O(h_\ell^2)$, is the fastest of the three. Further, they show that the MLMC (Mls)'s convergence of both V_ℓ and $E[\widehat{P}_\ell - \widehat{P}_{\ell-1}]$ is the second fastest of the three. The top left plot of Figure 13 shows that the SMC (Tlr), the SMC (Mls), and the SMC (Elr) have about the same variance, $V[\widehat{P}_\ell]$. For $l = 3$, the V_ℓ of the MLMC (Tlr) is more than 10,000,000 times smaller than $V[\widehat{P}_\ell]$, and is more than 100 times smaller than the V_ℓ of the MLMC (Mls), and is more than 10,000 times smaller than the V_ℓ of the MLMC (Elr). Figure 14 shows the computational cost of MLMC and SMC. Compared with the three SMC methods, the three MLMC methods significantly reduce computational cost, respectively. The two bottom plots of Figure 13 show that the MLMC (Tlr) needs the smallest computational complexity to achieve required accuracy ϵ. Compared with the MLMC (Mls), the MLMC (Tlr) attains a slight computational cost reduction of approximately 7% for $\epsilon = 5.0 \times 10^{-5}$.

3.2.4. Exchange option

The Exchange option discounted payoff is given by

$$F = \exp(-rT)\max\left(S_T^1 - S_T^2, 0\right) \tag{3.1}$$

where $\{S_t^1\}_t$ and $\{S_t^2\}_t$ are two geometric Brownian motions with constants r, q_1, q_2, v_1, and v_2

$$dS_t^1 = (r - q_1)\, S_t dt + v_1\left(S_t^1, t\right) S_t dW_t^1, \qquad 0 < t < T,$$
$$dS_t^2 = (r - q_2)\, S_t dt + v_2\left(S_t^2, t\right) S_t dW_t^2, \qquad 0 < t < T.$$

where $\{W_t^1\}_t$ and $\{W_t^2\}_t$ are correlated with $dW_t^1 dW_t^2 = \rho dt$ with $\rho \in [-1, 1]$. We define $\{U_t\}_t \equiv \{S_t^1/S_t^2\}_t$. (3.1) can be rewritten as follows.

$$\begin{aligned} F &= \exp(-rT)\max\left(S_T^1 - S_T^2, 0\right) \\ &= S_{t_0}^2 exp(-q_2 T)\max\left(S_T^1/S_T^2 - 1, 0\right) \\ &= S_{t_0}^2 exp(-q_2 T)\max\left(U_T - 1, 0\right), \end{aligned}$$

where $\{U_t\}_t$ follows a geometric Brownian motion

$$dU_t = (q_2 - q_1)U_t dt + v^* U_t dW_t^*, \qquad 0 \le t < T \tag{3.2}$$

with $v^* \equiv \sqrt{v_1^2 + v_2^2 - 2\rho_{1,2} v_1 v_2}$ (see Villani [15]). We simulate the discretization of (3.2) to price this Exchange option. The fine level and the coarse level discounted payoffs are calculated by

$$\begin{aligned} \widehat{P}_\ell^{f,i} &= \exp(-q_2 T)\widehat{S}_{M^\ell}^{2,f,i}\max(0, \widehat{U}_{M^\ell}^{f,i} - K), \quad i = 1, 2, \ldots, N_\ell, \\ \widehat{P}_{\ell-1}^{c,i} &= \exp(-q_2 T)\widehat{S}_{M^\ell}^{2,c,i}\max(0, \widehat{U}_{M^\ell}^{c,i} - K), \quad i = 1, 2, \ldots, N_\ell. \end{aligned}$$

We set $q_1 = 0.05$, $q_2 = 0.04$, $v_1 = 0.2$, $v_2 = 0.3$, and $\rho = 0.4$. The result denotes the same tendency as the Cliquet option case. The two top plots of Figure 15 show that the MLMC (Tlr)'s convergence of both V_ℓ and $E[\widehat{P}_\ell - \widehat{P}_{\ell-1}]$, $O(h_\ell^3)$ and $O(h_\ell^2)$, is the fastest of the three. Moreover, they show that the MLMC (Mls)'s convergence of both V_ℓ and $E[\widehat{P}_\ell - \widehat{P}_{\ell-1}]$ is the second fastest of the three. The top left plot of Figure 15 shows that the SMC (Tlr), the SMC (Mls), and the SMC (Elr) have about same variance, $V[\widehat{P}_\ell]$. For $\ell = 3$, the V_ℓ of the MLMC (Tlr) is more than 1,000,000 times smaller than $V[\widehat{P}_\ell]$, and is more than 100 times smaller than the V_ℓ of the MLMC (Mls), and is more than 10,000 times smaller than the V_ℓ of the MLMC (Elr). Figure 16 shows the computational cost of MLMC and SMC. Compared with the SMC (Elr), the SMC (Mls), and the SMC (Tlr), the MLMC (Elr), the MLMC (Mls), and the MLMC (Tlr) significantly reduce computational cost, respectively. The two bottom plots of Figure 15 show that the MLMC (Tlr) needs the smallest computational cost to achieve required accuracy ϵ. Compared with the MLMC (Mls), the MLMC (Tlr) attains a computational cost reduction of about 20%.

3.3. Vanilla option valuation by MLMC method based on the SABR model

The original SABR model was proposed by Hagan, Kumar, Lesniewski, and Woodward[10]. As with the Heston model, which was tested by the MLMC (Elr) by Giles [3], the SABR model is a very well-known stochastic volatility model in both academic and practical fields. In particular, the SABR model is used in many financial institutions, since the model can capture the correct dynamics of the volatility smile in derivatives markets. We treat the following SABR model (see Tian, Zhu, Klebaner, and Hamza[14]), which is obtained by applying Ito's lemma to the original model,

$$dS_t = rS_t dt + \alpha_t D(t,T)^{1-\beta} S_t^\beta dW_t^1, \qquad 0 \le t < T, \tag{3.3}$$

$$d\alpha_t = \nu \alpha_t dW_t^2, \qquad 0 \le t < T, \tag{3.4}$$

with constants $r, \nu > 0$ and $\beta \in [0, 1]$, where $D(t,T) = \exp\left(-\int_t^T r(s)ds\right)$, and geometric Brownian motions $\{W_t^1\}_t$ and $\{W_t^2\}_t$ are correlated with $dW_t^1 W_t^2 = \rho dt$ for some $\rho \in [-1, 1]$.

The corresponding discretizations of (3.3) and (3.4) are given by

$$\widehat{S}_{t_{n+1}} - \widehat{S}_{t_n} = r\widehat{S}_{t_n}\Delta t + \widehat{\alpha}_{t_n} exp\left((T-t_n)(\beta-1)\right)\widehat{S}_{t_n}^{\beta}\Delta W_{t_n}^1,$$
$$n = 0, 1, \ldots, D-1,$$
$$\widehat{\alpha}_{t_{n+1}} - \widehat{\alpha}_{t_n} = \nu\widehat{\alpha}_{t_n}\left(\rho\Delta W_{t_n}^1 + \sqrt{1-\rho^2}\Delta W_{t_n}^2\right), \qquad n = 0, 1, \ldots, D-1,$$

where $\Delta W_{t_n}^k = W_{t_{n+1}}^k - W_{t_n}^k, k = 1, 2$. As with the Heston stochastic volatility model in Giles [3], we cannot obtain theoretical results of the order of both strong and weak convergence, as the volatility process $\{\alpha_t\}_t$ of the SABR model does not satisfy a global Lipschitz condition. We set $\hat{\alpha}_0 = 0.2$, $\beta = 0.5$, $\rho = 0.4$, and $\nu = 0.4$. The top left plot of Figure 17, however, numerically suggests that strong convergence is a little slower than the first order, $O(h_\ell)$. The top right plot suggests that weak convergence is faster than the second order, $O(h_\ell^2)$. As with the Heston model case in Giles [3], the MLMC method is superior to the SMC method under the SABR model, since the bottom right plot shows that the MLMC (Elr) attains a computational cost reduction of about 75-90% compared to the SMC (Elr).

4. Concluding Remarks and Future Studies

In this study, we have numerically demonstrated the performance of the MLMC method using the Euler scheme, the Milstein scheme, and the order 1.5 Taylor strong scheme for options pricing. We first test the MLMC (Tlr) for European vanilla, Asian, Lookback, and Digital options based on a simple geometric Brownian motion. Second, we compare the numerical performance of the MLMC (Tlr), the MLMC (Mls), and the MLMC (Elr) for Power, Rainbow, Cliquet, and Exchange options based on a simple geometric Brownian motion, and finally, test the MLMC (Elr) for the European vanilla option based on the SABR model. All the numerical results show that the MLMC method has much better performance than the SMC method. The MLMC (Tlr) greatly reduces computational complexity (up to 99.9%) compared to other standard and multilevel Monte Carlo methods such as the SMC (Elr), the SMC (Mls), the SMC (Tlr), and the MLMC (Elr). In addition, the MLMC (Tlr) achieves a computational complexity reduction of up to 20% compared to the MLMC (Mls). A direction that future studies may take is the theoretical analysis of the MLMC (Tlr). The MLMC (Elr) was theoretically studied by Giles[3] for Lipschitz payoff case and by Giles, Desmond, and Higham[5] for non-Lipschitz payoff case under global Lipschitz bounds. The theoretical analysis of the MLMC (Mls) was studied by Giles, Debrabant, and Rößler[8] under certain standard conditions such as a uniform Lipschitz condition, a linear growth bound, and an additional Lipschitz conditon. Furthermore, the conditions under which the order 1.5 Taylor strong scheme actually attains the order 1.5 of strong convergence is discussed in Theorem 10.6.3 by Kloeden and Platen[12]. Thus, a theoretical analysis of the MLMC (Tlr) for pricing the above-mentioned eight options should be studied on the basis of both the theorem in Kloeden and Platen[12] and the conditions assumed in previous studies.

References

[1] Dick, J., Kuo, F. Y., Gla, T. Le.and Schwab, C. (2016). Multilevel Higher Order QMC Petrov–Galerkin Discretization for Affine Parametric Operator Equations, *SIAM Journal on Numerical Analysis*, **54** (5), 2541-2568.

[2] Giles, M. B. (2008). Improved multilevel Monte Carlo convergence using the Milstein scheme, In *Monte Carlo and Quasi-Monte Carlo Methods 2006*, (Edited by Keller, A., Heinrich, S. and Niederreiter, H.), 343-358, Springer-Verlag, Berlin.

[3] Giles, M. B. (2008). Multilevel Monte Carlo path simulation, *Operations Research*, **56** (3), 607-617.

[4] Giles, M. B. and Waterhouse, L. (2009). Multilevel quasi-Monte Carlo path simulation, In *Advanced Financial Modeling*, (Edited by Albrecher, H., Runggldier, W. and Schachermayer, W.), Radon Series on Computational and Applied Mathematics **8**, 165-181. De Gruyter.

[5] Giles, M. B., Higham, D. J. and Mao, X. (2009). Analysing multi-level Monte Carlo for options with non-globally Lipschitz payoff, *Annals of Applied Probability*, **13** (3), 1585-1620.

[6] Giles, M. B. and Szpruch, L. (2013). Antithetic multilevel Monte Carlo estimation for multidimensional SDEs, In *Monte Carlo and Quasi-Monte Carlo Methods 2012*, (Edited by DICK, J., KUO, F. Y., Peters G. W. and Sloan, I. H.), 367-384, Springer.

[7] Giles, M. B. and Szpruch, L. (2014). Antithetic multilevel Monte Carlo estimation for multi-dimensional SDEs without Lévy area simulation, *Finance Stoch*, **24** (4), 403-413.

[8] Giles, M. B., Debrabant, K. and Rößler, A. (2013). Numerical analysis of multilevel Monte Carlo path simulation using the Milstein discretisation, preprint, arXiv:1302.4676.

[9] Glasserman, P. (2004). *Monte Carlo Methods in Financial Engineering*, Springer-Verlag, New York.

[10] Hagan, P. S., Kumar, D., Lesniewski, A. and Woodward, D. E. (2002) Managing smile risk. *Wilmott Magazine* September 2002, 84-08.

[11] Kebaier, A. and Lelong, J. (2013). Coupling Importance Sampling and Multilevel Monte Carlo using Sample Average Approximation, preprint, arXiv:1510.03590v2.

[12] Kloeden, P. E. and Platen, E. (1999). *Numerical Solution of Stochastic Differential Equations* 3rd edition, Springer-Verlag, Berlin.

[13] Nobile, F. and Tesei, F. (2015). A Multi Level Monte Carlo method with control variate for elliptic PDEs with log-normal coefficients, *Stochastic Partial Differential Equations: Analysis and Computations*, **3** (3), 398-444.

[14] Tian, Y., Zhu, Z., Klebaner, F. C., and Hamza, K. (2012). Pricing barrier and American options under the SABR model on the graphics processing unit, *CONCURRENCY AND COMPUTATION: PRACTICE AND EXPERIENCE*, **24**, 867-879.

[15] Villani, G. (2010). A Monte Carlo approach to value exchange options using a single stochastic factor, In *Mathematical and Statistical Methods for Actuarial Sciences and Finance*, (Edited by Corazza, M. and Pizzi, C.), 305-314, Springer-Verlag, Italia.

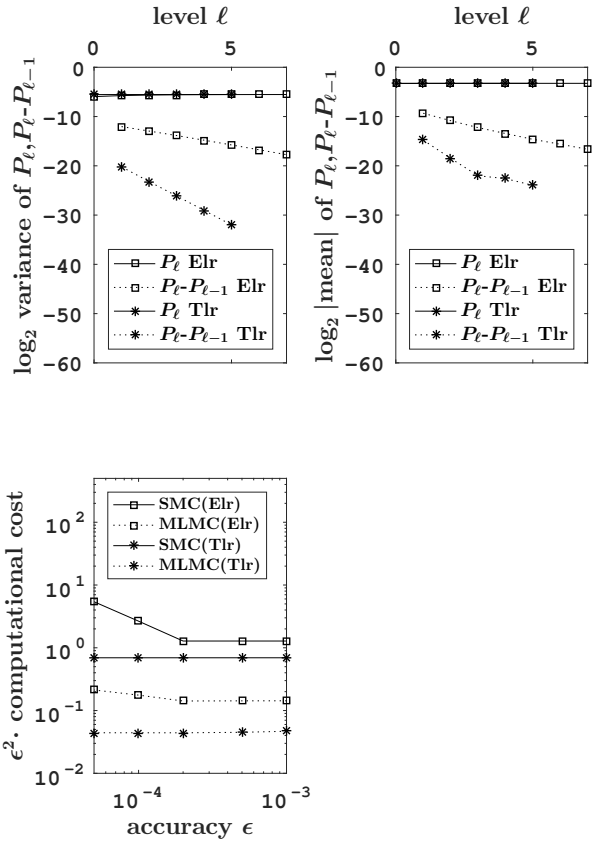

Figure 1: European vanilla option (option price: 0.10)

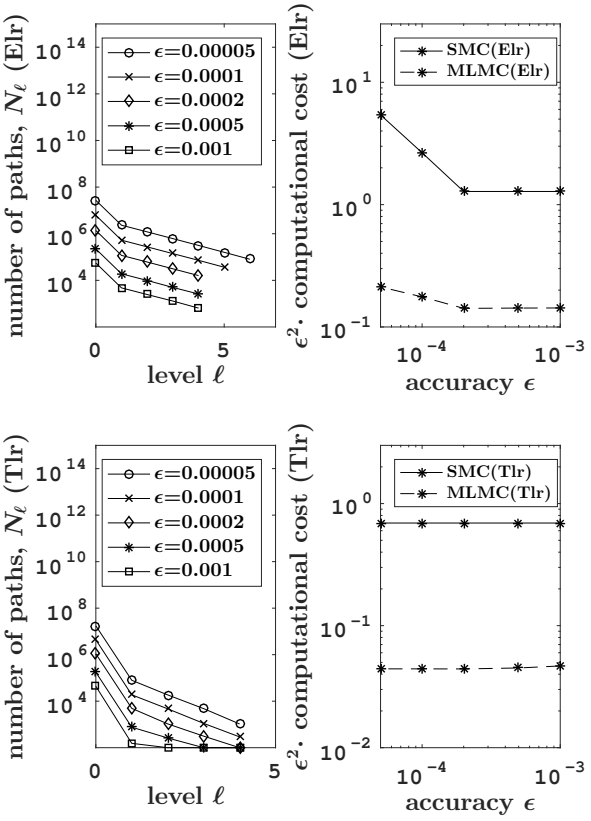

Figure 2: European vanilla option (option price: 0.10)

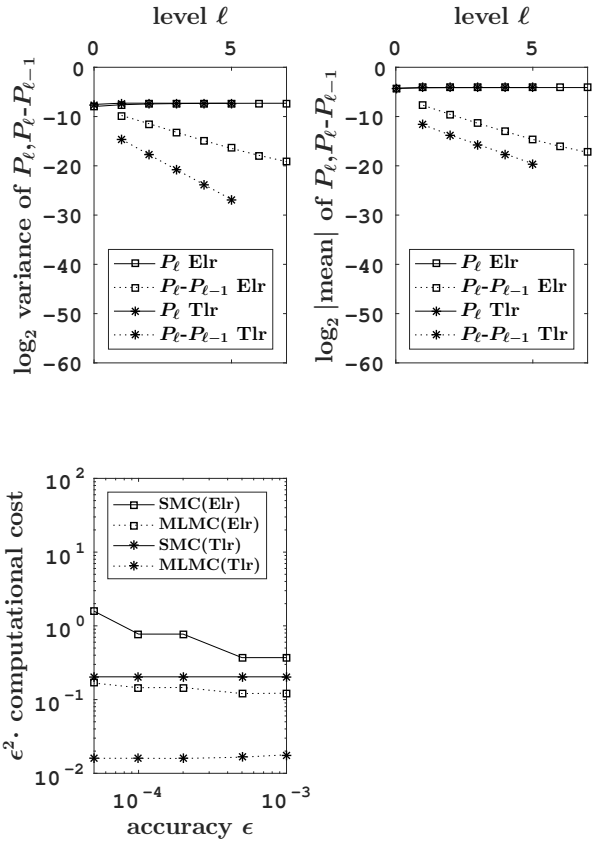

Figure 3: Asian option (option price: 0.058)

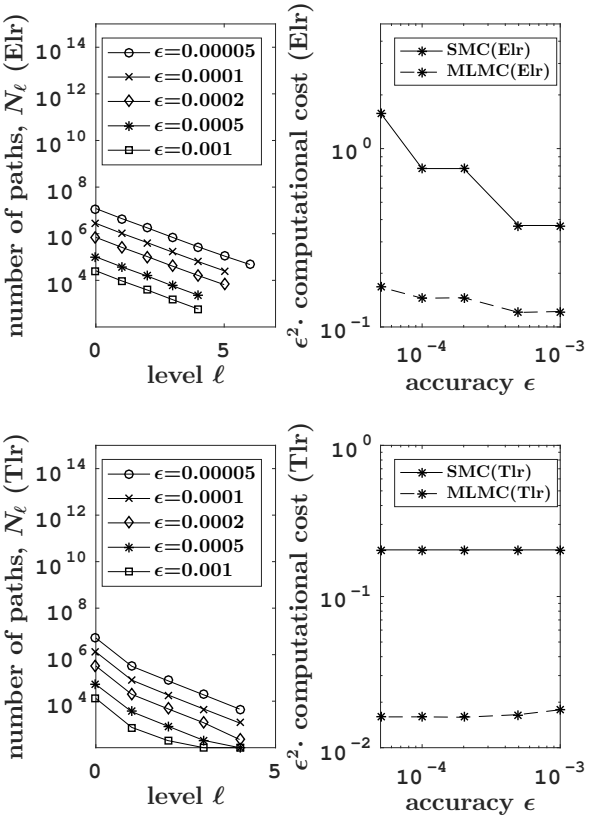

Figure 4: Asian option (option price: 0.058)

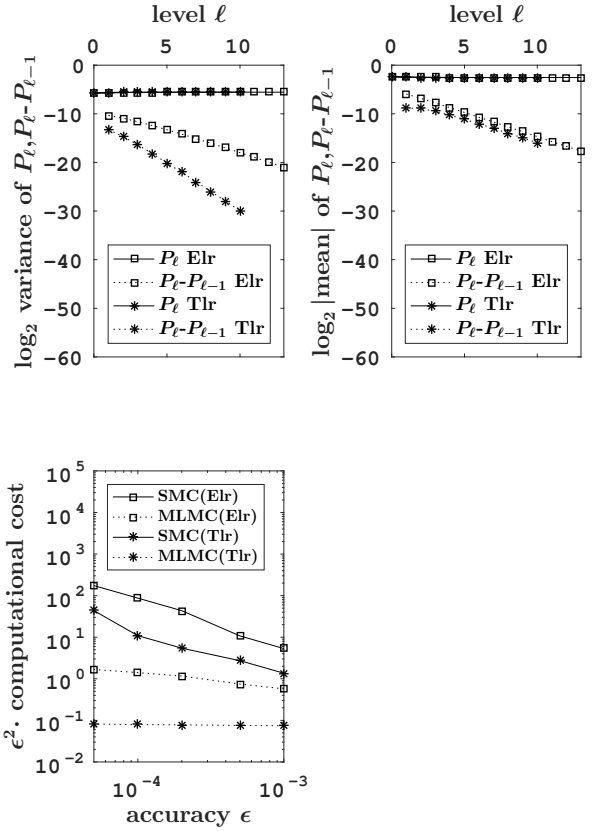

Figure 5: Lookback option (option price: 0.17)

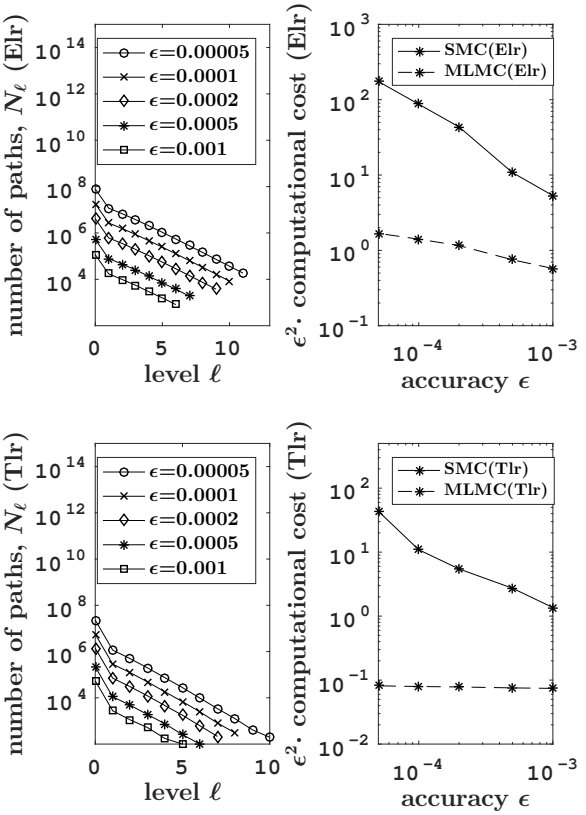

Figure 6: Lookback option (option price: 0.17)

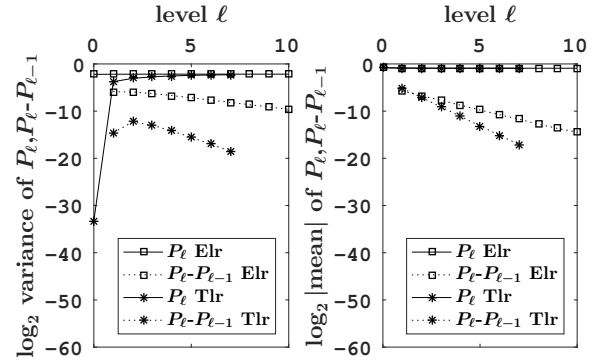

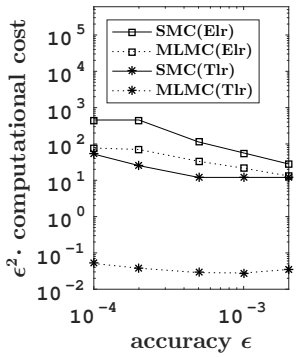

Figure 7: Digital option (option price: 0.53)

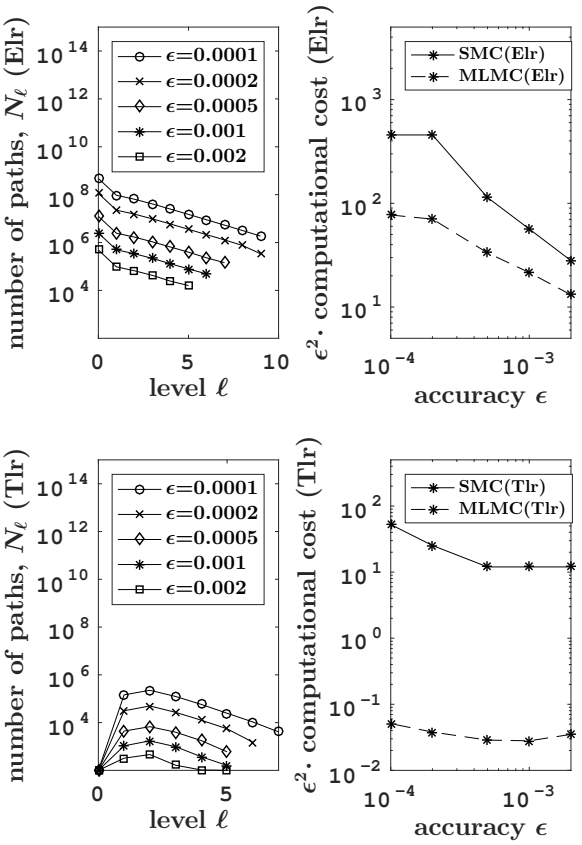

Figure 8: Digital option (option price: 0.53)

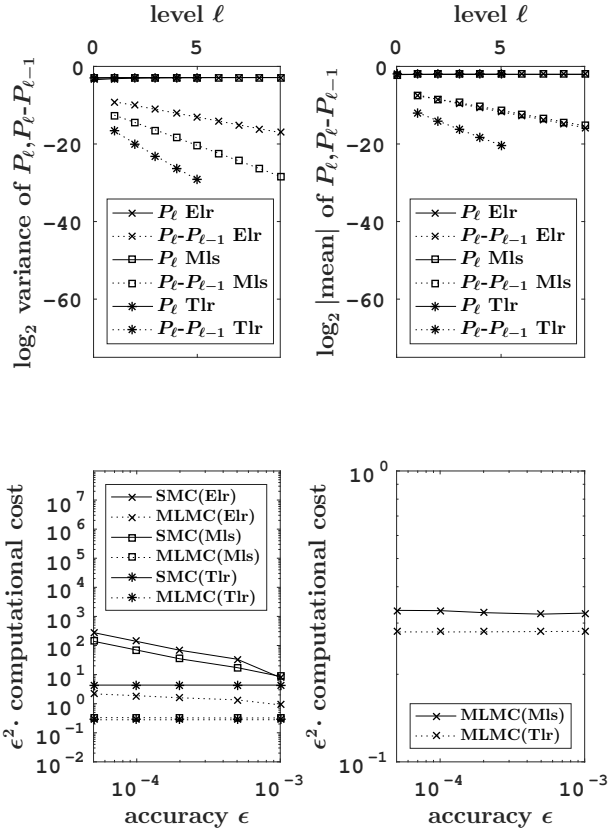

Figure 9: Power option (option price: 0.24)

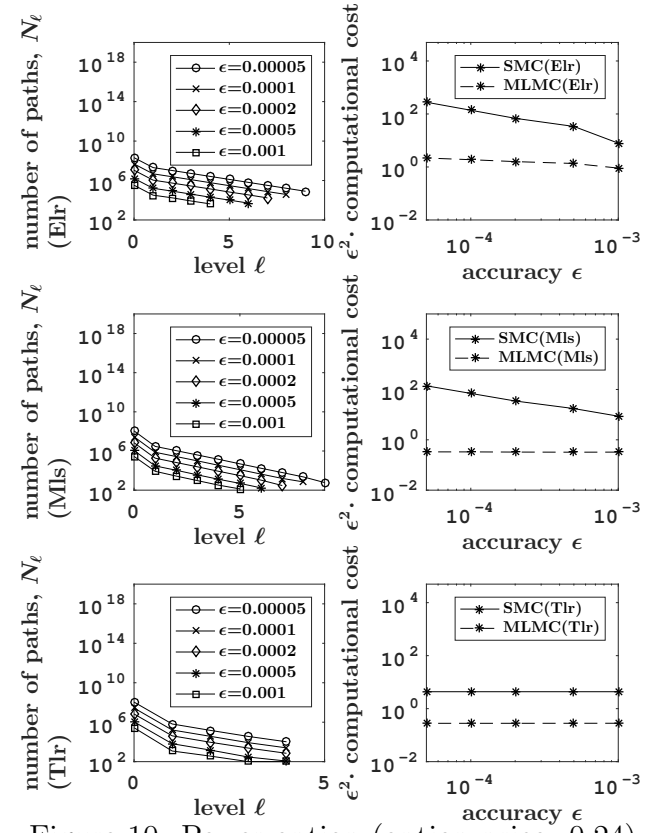

Figure 10: Power option (option price: 0.24)

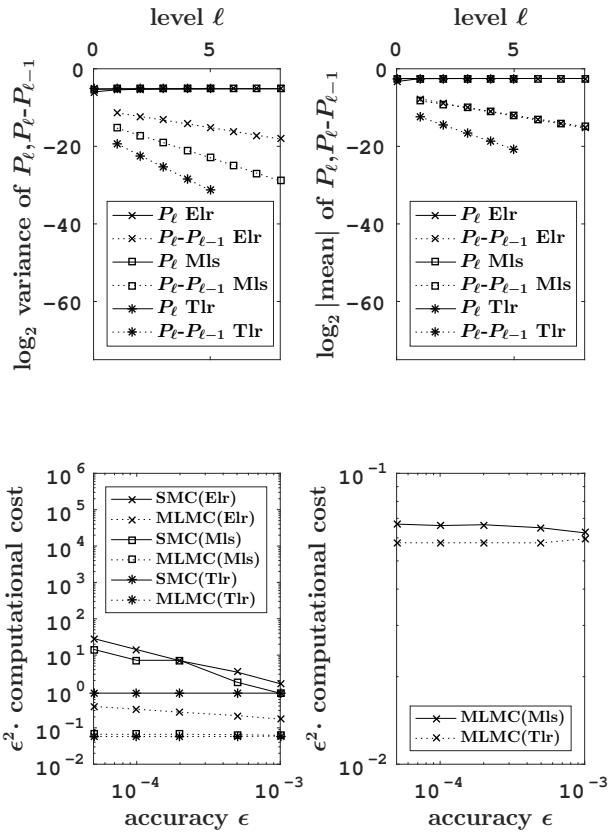

Figure 11: Rainbow option (option price: 0.18)

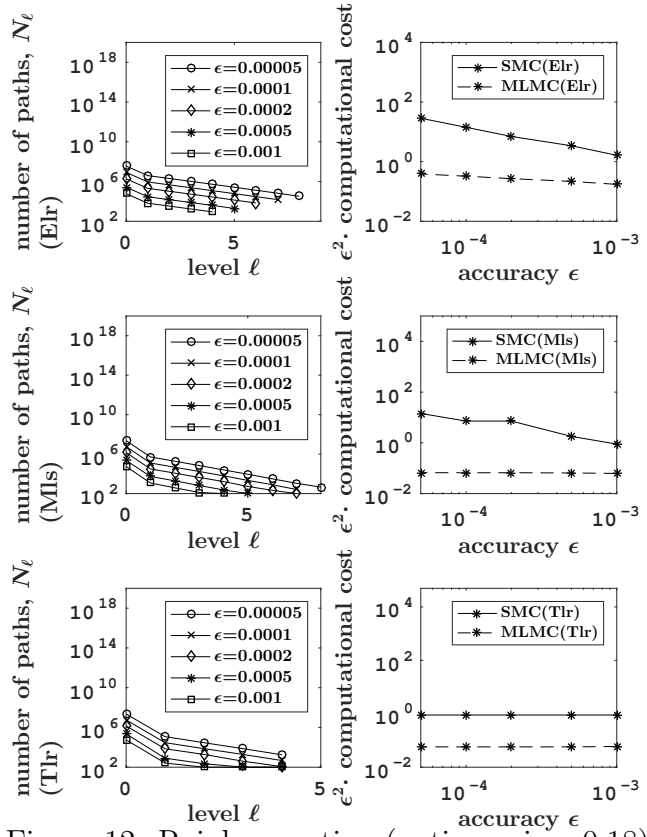

Figure 12: Rainbow option (option price: 0.18)

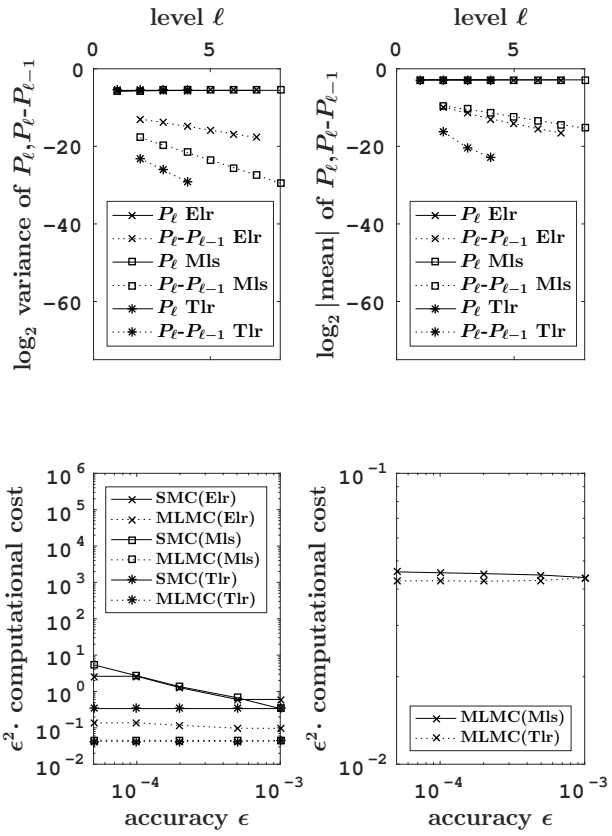

Figure 13: Cliquet option (option price: 0.14)

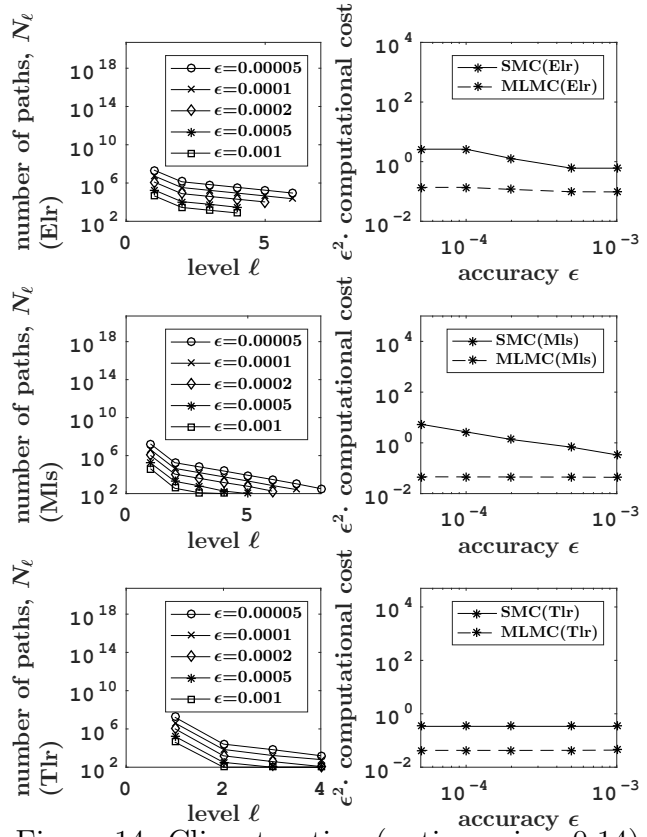

Figure 14: Cliquet option (option price: 0.14)

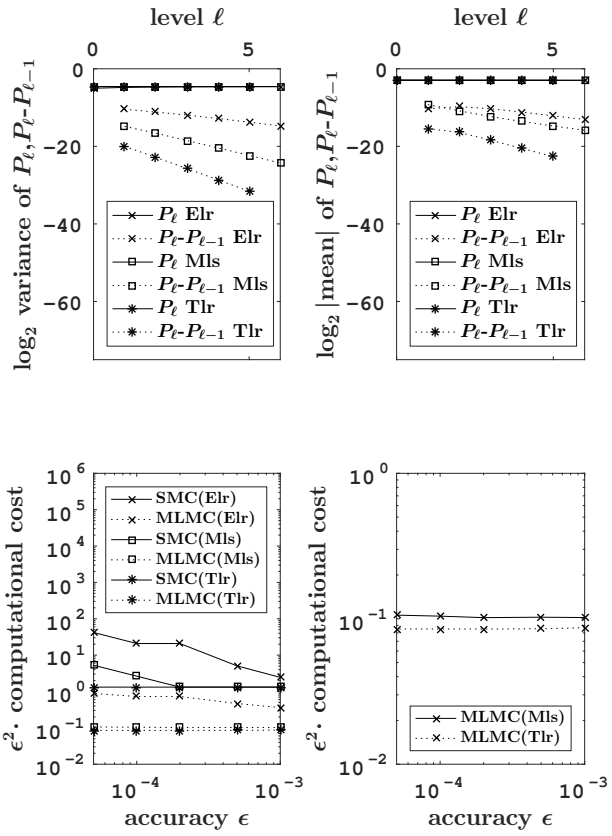

Figure 15: Exchange option (option price: 0.13)

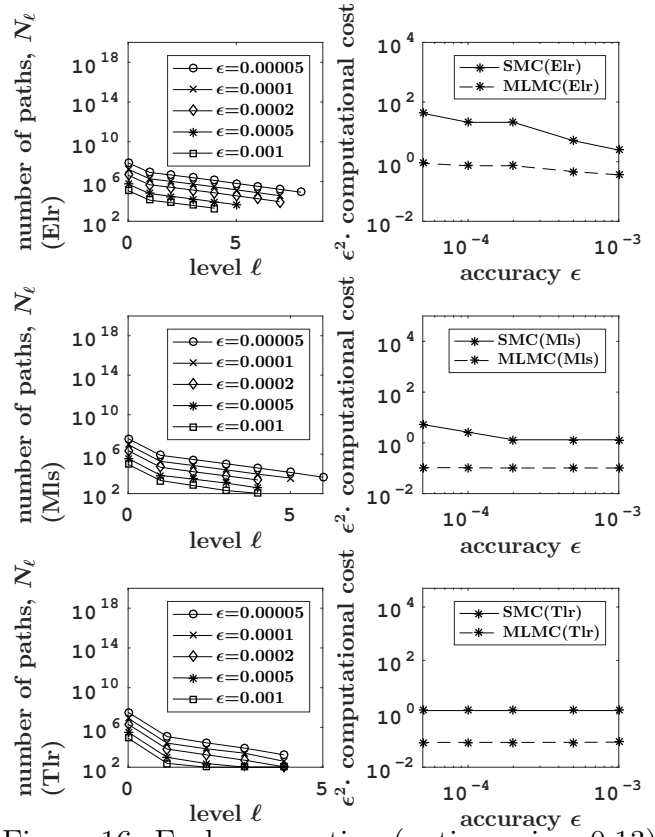

Figure 16: Exchange option (option price: 0.13)

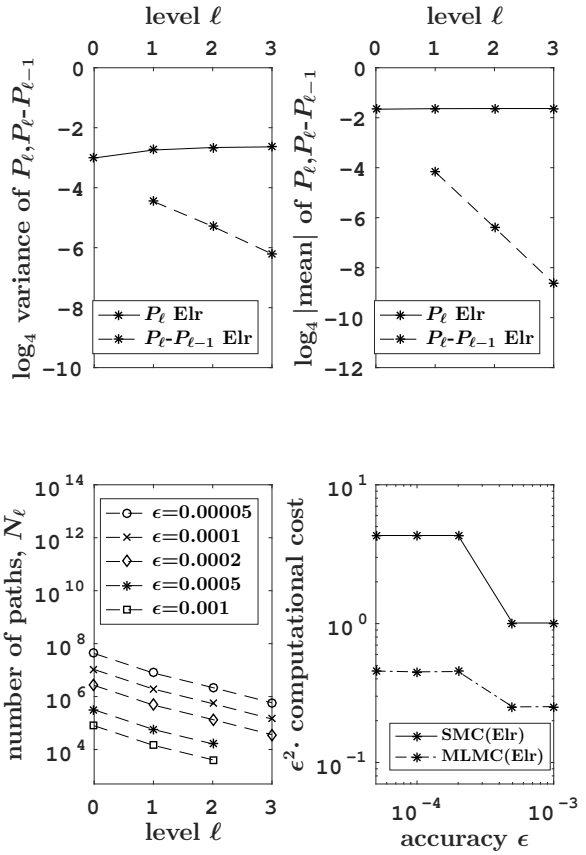

Figure 17: European vanilla option based on SABR model (option price: 0.10)

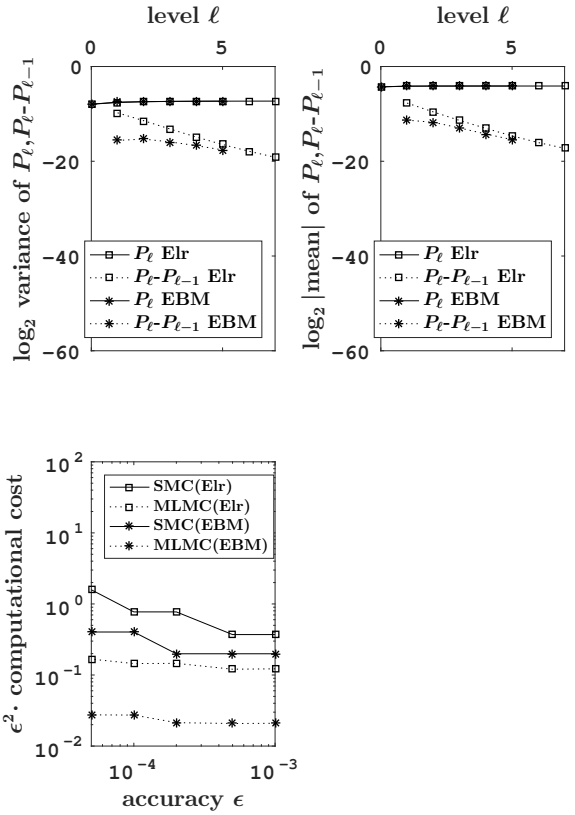

Figure 18: Asian option (option price: 0.058)

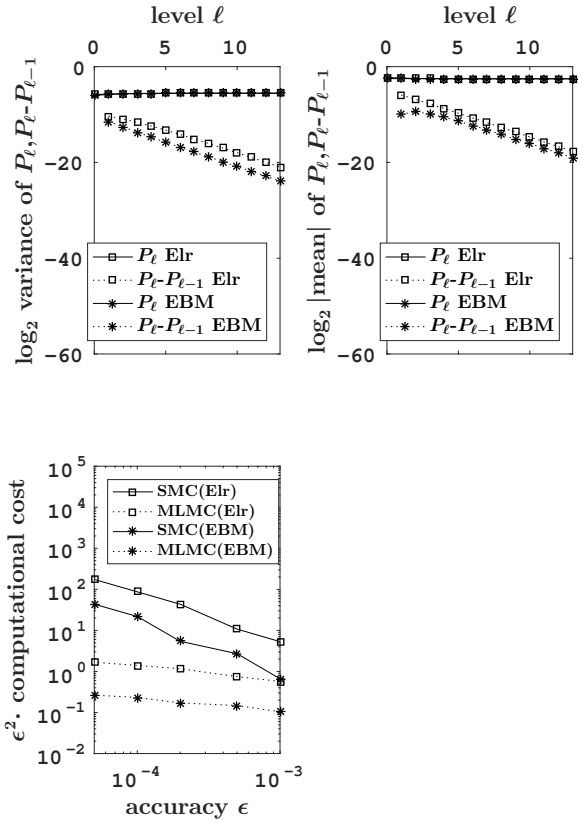

Figure 19: Lookback option (option price: 0.17)

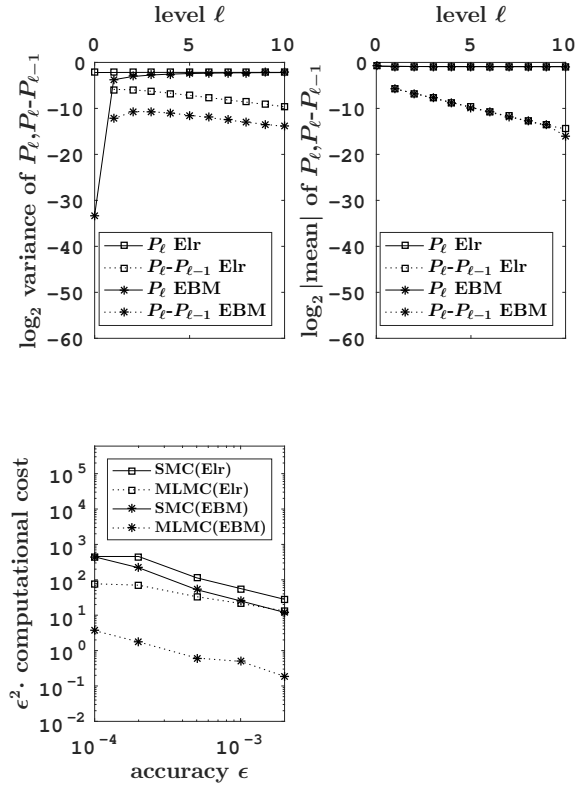

Figure 20: Digital option (option price: 0.53)